



**13<sup>TH</sup> CANADIAN MASONRY SYMPOSIUM**  
**HALIFAX, CANADA**  
**JUNE 4<sup>TH</sup> – JUNE 7<sup>TH</sup> 2017**



---

**PROPOSED BACKBONE MODEL FOR REINFORCED MASONRY BUILDINGS  
WITHOUT AND WITH BOUNDARY ELEMENTS**

**Ezzeldin, Mohamed<sup>1</sup>; El-Dakhkhni, Wael<sup>2</sup> and Wiebe, Lydell<sup>3</sup>**

**ABSTRACT**

The development of nonlinear models, which describe the inelastic behavior of the individual components of a building at different performance levels (e.g. life safety and collapse prevention), is an essential step to perform the nonlinear static analyses recommended in North American codes and standards (e.g. ASCE/SEI 41). However, current methodologies for generating nonlinear models of reinforced masonry (RM) buildings do not adequately account for various system-level aspects, such as the out-of-plane rigidity of the floor slab. Many studies have shown that these aspects would significantly change the overall building response under seismic loading. In addition, although North American codes and standards define demand parameters of RM shear walls with *rectangular* cross sections through a standardized backbone relationship between forces and deformations, no corresponding values are given for RM shear walls with boundary elements. To address these issues, this study proposes an approach for generation of backbone models of RM shear wall buildings without and with boundary elements. The experimentally validated modeling approach shows the importance of including the out-of-plane stiffness of the floor diaphragms when estimating the overall building performance. Finally, the experimental and numerical responses are compared in terms of the most relevant characteristics, including the initial stiffness, peak load, and stiffness and strength degradation, in an effort to present a useful system-level response prediction tool for the nonlinear static procedure.

**KEYWORDS:** *backbone model, nonlinear analysis, reinforced masonry, system-level behavior*

---

<sup>1</sup> Postdoctoral Fellow, Department of Civil Engineering, McMaster University, Hamilton, ON, L8S 4L7, Canada, ezzeldms@mcmaster.ca

<sup>2</sup> Martini Mascarin and George Chair in Masonry Design, Department of Civil Engineering, McMaster University, Hamilton, ON, L8S 4L7, Canada, eldak@mcmaster.ca

<sup>3</sup> Assistant Professor, Department of Civil Engineering, McMaster University, Hamilton, ON, L8S 4L7, Canada, wiebel@mcmaster.ca

## INTRODUCTION

The studies that have been conducted to develop nonlinear models for reinforced masonry (RM) shear walls can be mainly categorized by the degree of model idealization as: (1) continuum finite element models, where the nonlinear behavior of the masonry, longitudinal and shear reinforcement that comprise the shear wall are modelled explicitly (e.g. Mojsilovic and Marti [1]); (2) distributed plasticity (fiber) models, where numerical integration is used through the RM shear wall cross section and along its length to distribute plasticity (e.g. Ezzeldin et al. [2]); and (3) concentrated plasticity models, where all the nonlinear effects of the RM shear walls are lumped into an inelastic spring idealized by a single-degree-of-freedom relationship (e.g. Marques and Lourenço [3]). Although continuum finite element and distributed plasticity models can accurately capture behaviors such as initiation of masonry cracking and steel yielding, they are nonetheless computationally intensive and have limited ability to capture strength degradation due to such factors as reinforcing bar buckling, bond slip, and shear failure [4]. Conversely, concentrated plasticity models can capture strength degradation effects and they do not require the level of detailed representation that is needed for both continuum finite element and distributed plasticity models.

Most of the modelling studies to date have been conducted on RM walls at the component level (i.e. individual wall), with only a few studies focused on system-level response evaluation of RM walls (i.e. complete building) (e.g., Priestley et al. [5]). Recently, several studies argued that there are specific system-level aspects (e.g. slab's in-plane and out-of-plane stiffness) that cannot be evaluated or assessed through component-level testing. For example, the in-plane slab stiffness results in different component-level strength and displacement demands from essentially identical RM shear walls [6]. In addition, Ashour et al. [6] conducted experimental programs that demonstrated that slab flexural out-of-plane coupling was an important system-level aspect that affected the overall RM building performance. This included affecting the building stiffness, lateral resistance capacity, and trend of stiffness degradation, which in turn would significantly alter the overall building response under seismic loading.

The nonlinear models described above have considered only walls with rectangular cross sections, whereas RM buildings with boundary elements are a newly proposed system within the Canadian Standards Association "Design of Masonry Structures" S304-14 [7]. RM shear walls with boundary elements are also included in the TMS 402/602-16 [8], but no modelling parameters are provided for such walls as a distinct seismic force resisting system. Boundary elements in RM shear walls enhance the overall seismic performance relative to traditional RM shear walls (i.e. with rectangular cross sections) because closed ties and multiple layers of vertical bars can be accommodated within the boundary elements, thus providing a confining reinforcement cage (Shedid et al. [9]; Banting and El-Dakhakhni [10]). The nonlinear models developed in this paper also account for RM buildings with boundary elements in order to facilitate the development of prescriptive design requirements, as recommended by the TMS 402/602-16 [8].

This paper develops a simplified numerical model in OpenSees [11], using the concentrated plasticity modeling approach, to simulate the behaviour of RM buildings without and with boundary elements. A description of the experimental programs that are used to validate the proposed modelling technique is presented, followed by a detailed description of the numerical model development. Finally, the developed numerical responses are compared with experimental results in terms of the most relevant characteristics, including the initial stiffness, peak load, and stiffness and strength degradation.

## EXPERIMENTAL PROGRAMS

Ashour et al. [6] tested a one-third scaled two-story asymmetrical RM shear wall building (referred to as *Building III* hereafter) under displacement-controlled quasi-static fully-reversed cyclic loading. *Building III* was composed of four traditional (i.e. no boundary elements) shear walls aligned along the loading the North-South direction (W1<sub>III</sub>, W2<sub>III</sub>, W5<sub>III</sub> and W8<sub>III</sub>), and four other walls aligned orthogonally along the East-West direction (W3<sub>III</sub>, W4<sub>III</sub>, W6<sub>III</sub> and W7<sub>III</sub>), as shown in Figure 1.

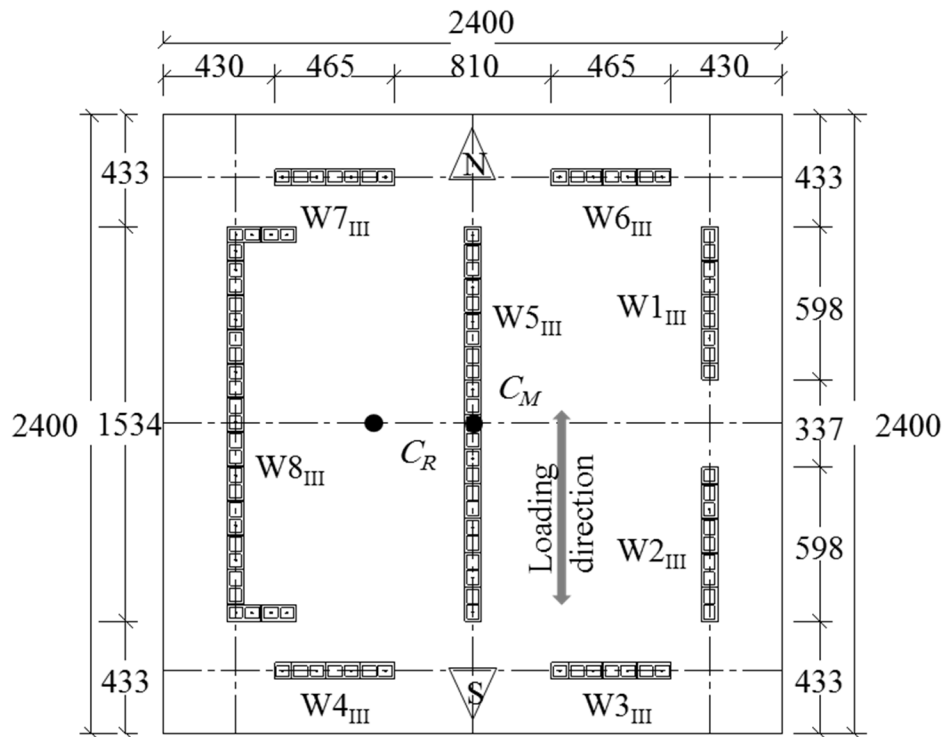


**Figure 1: Typical Plan Wall Configuration of *Building III* (Ashour et al. [6]), All Dimensions are in (mm).**

Ezzeldin et al. [12] tested a similar building with the same nominal strength (to allow for direct comparison with *Building III*), referred to as *Building IV* hereafter. The RM shear walls located along the loading direction in *Building III* were replaced in *Building IV* by RM shear walls with confined boundary elements (W1<sub>IV</sub>, W2<sub>IV</sub>, W5<sub>IV</sub> and W8<sub>IV</sub>), as shown in Figure 2. The boundary

elements were adopted in *Building IV* because they allow closed ties to be used and multiple layers of vertical reinforced bars to be accommodated, thus providing a confining reinforcement cage.

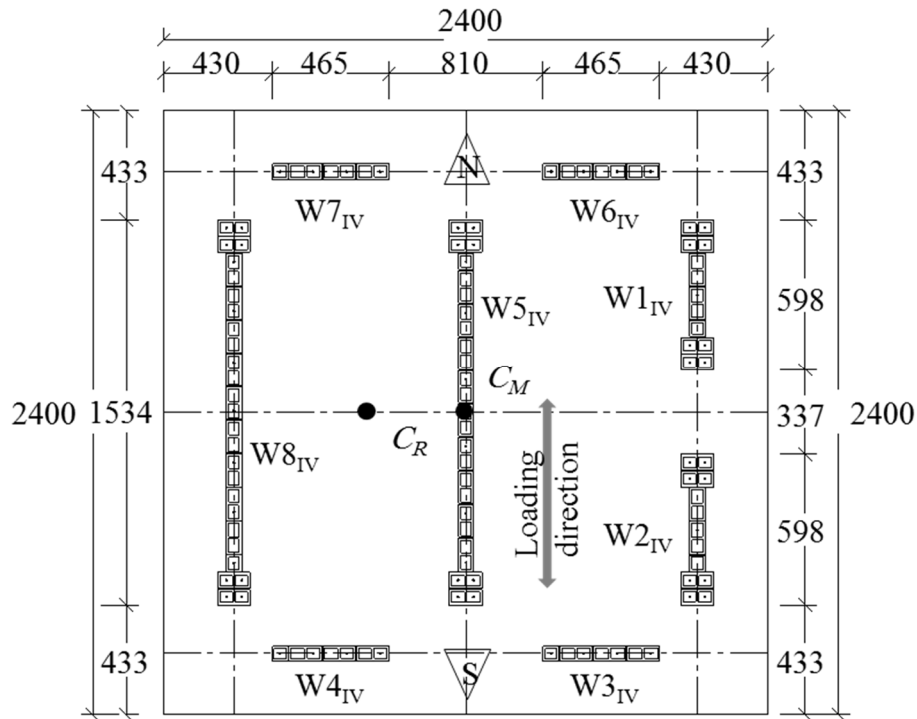


**Figure 2: Typical Plan Wall Configuration of *Building IV* (Ezzeldin et al. [12]), All Dimensions are in (mm).**

The asymmetrical wall configuration with respect to the loading direction in both buildings produced an eccentricity between the building floor Center of Mass,  $C_M$ , and the building Center of Rigidity,  $C_R$ , at the roof level, as shown in Figures 1 and 2. This engaged the torsional response of the building under the applied lateral loads. The overall scaled height of both buildings was 2,160 mm, comprising two floors, each 1,000 mm high (corresponding to 3,000 mm in full-scale), and reinforced concrete (RC) floors, each with dimensions of 2,400 mm  $\times$  2,400 mm in plan and 80 mm thick, as shown in Figure 3 for *Building IV*. Full details of the experimental programs can be found in Ashour et al. [6] and Ezzeldin et al. [12] for *Buildings III* and *IV*, respectively.

## REINFORCED MASONRY NONLINEAR MODELING

### *Current ASCE/SEI 41-13 Backbone Modeling Approach*

ASCE/SEI 41-13 [13] provides standardized load-drift backbone relationship for RM shear walls, as shown in Figure 4, where there is an elastic range from point A (unloaded point) to point B (effective yield point) and a plastic range from point B to points C (ultimate strength

point) and D (strength degradation point). At deformation levels greater than that corresponding to point D, the RM shear wall strength is essentially zero.

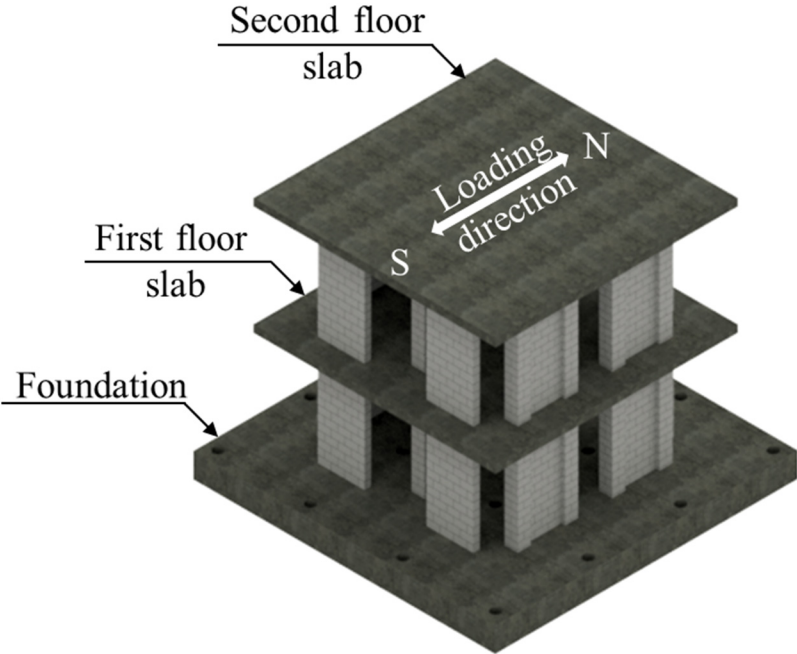


Figure 3: Three-Dimensional (3-D) representation of *Building IV* (Ezzeldin et al. [12]).

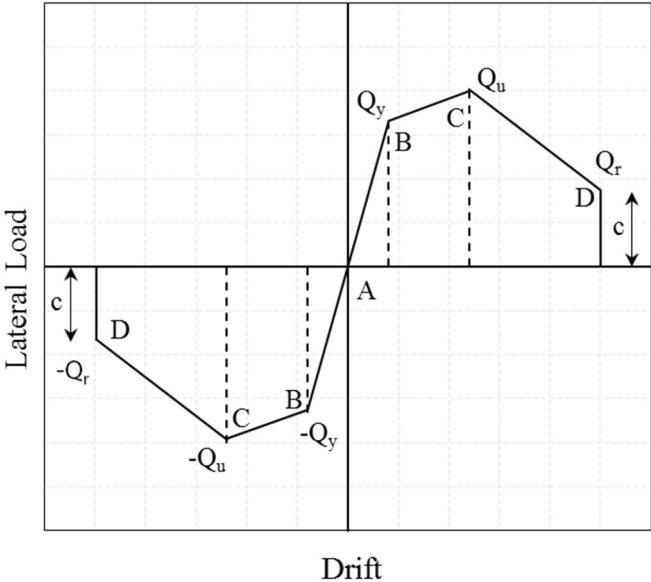
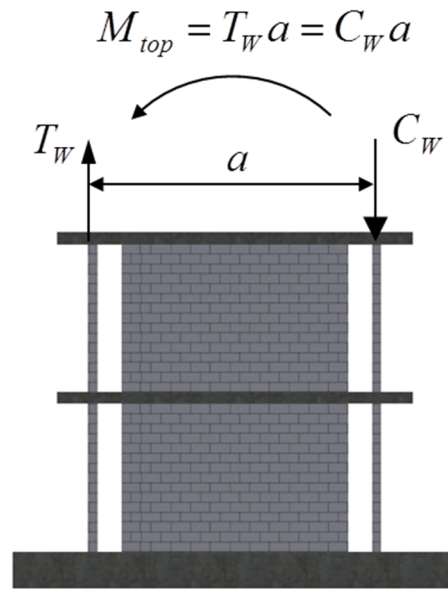


Figure 4: Simplified ASCE/SEI 41-13 load-drift relationship for RM shear walls [13].

Figure 4 shows that there are three key points needed to determine the individual wall response. For the yield strength,  $Q_y$ , a linear strain profile is used to calculate the yield moment,  $M_y$ , with a

yield strain of the outermost steel reinforcement set to 0.0025. To calculate the wall ultimate strength,  $Q_u$ , based on the ultimate moment,  $M_u$ , the ultimate masonry strain is taken as 0.0025, as specified by the TMS 402/602-16 [8]. Finally, the residual strength value,  $Q_r$ , is calculated by multiplying  $Q_u$  by the parameter “ $c$ ” specified in ASCE/SEI 41-13 [13]. For all three strength calculation cases, a bending moment diagram was assumed to relate the moment to the lateral load. This diagram was selected based on the results of both experimental programs (i.e. *Building III* and *Building IV*), which showed the significant effect of the diaphragm coupling in terms of changing the system-level response of the RM shear walls aligned along the main direction of loading. More specifically, the orthogonal walls (W3 and W4 or W6 and W7) resulted in a coupling moment at the top level,  $M_{top}$ , due to the effect of tension force developed at yielding of the reinforcement,  $T_w$ , in one pair of the orthogonal walls and an equal compression force,  $P_w$ , in the other pair of the orthogonal walls. As such, the coupling moment,  $M_{top}$ , is equal to the tension or compression force in one pair of the orthogonal walls multiplied by the distance,  $a$ , between the orthogonal walls, as shown in Figure 5. However, the diaphragm coupling decreases at higher drift levels due to the cracks developed within the diaphragm, until the walls respond almost as cantilevers at large drifts. As a simplification of this behavior, the walls aligned along the loading direction in both buildings are assumed to have  $M_{top}$  at the top level, until reaching the ultimate point (i.e. point C). At point E, the walls are assumed to be unrestrained by the slab at the top level.



**Figure 5: Development of Coupling Moment ( $M_{top}$ ) at the Top Level at points B and C.**

### ***Proposed Numerical Backbone Model***

A simplified numerical model is developed in this paper using OpenSees [11] and validated against the experimental results of *Buildings III* and *IV*. The developed numerical model adopts a concentrated plasticity approach, where elastic beam-column elements are used to model the

walls of both buildings, with the wall inelastic behavior is modelled by a zero-length inelastic rotational spring at the base of each wall, as shown in Figure 6. These springs follow a bilinear hysteretic response based on the modified Ibarra-Medina-Krawinkler deterioration model with pinching hysteretic response (Ibarra et al. [14], ModIMKPinching material in OpenSees).

The model is represented by a moment-rotation relationship that depends on the yield moment,  $M_y$ , the ultimate moment,  $M_u$ , the coupling moment,  $M_{top}$ , the residual moment,  $M_r$ , the ultimate plastic rotation,  $\theta_u$ , the residual plastic rotation,  $\theta_r$ , and the rotational stiffness,  $K_\theta$ . The parameters  $M_y$ ,  $M_u$ ,  $M_{top}$  and  $M_r$  were defined earlier, while  $\theta_u$  and  $\theta_r$  are provided in ASCE/SEI 41-13 [13] for reinforced concrete (RC) shear walls, but no corresponding values are currently given for RM shear walls. As such, the parameters specified for RC walls were used to predict the response of the individual shear walls in *Buildings III* ( $a=0.006$  rad,  $b=0.015$  rad and  $c=60\%$ ) and *IV* ( $a=0.01$  rad,  $b=0.02$  rad and  $c=75\%$ ). This approach was considered acceptable during the model development because fully grouted RM structural wall construction is very similar to RC structural wall construction in terms of the material behavior and the analysis of displacements [9, 10], and because it will be shown later in this paper to produce reasonable results.

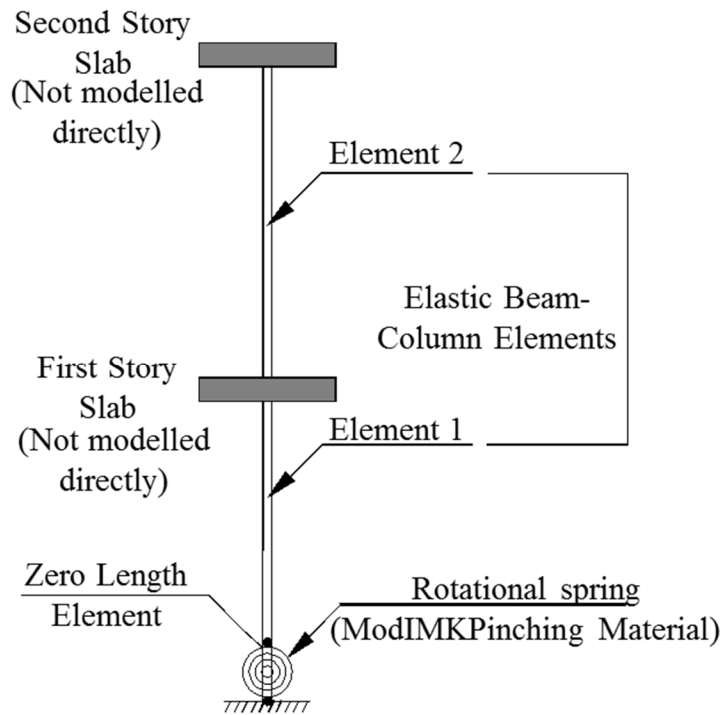


**Figure 6: Schematic Diagram of the Numerical Model.**

The rotational stiffness,  $K_\theta$ , can be calculated from Equation (1) in terms of the wall height,  $h$ , and the wall effective moment of inertia,  $I_e$ ,

$$K_\theta = \frac{(n+1)6EI_e}{h} \quad (1)$$

Equation (2) was used to calculate  $I_e$ , according to Paulay and Priestley [15], where  $\alpha$  is a reduction factor,  $A_g$  is the gross masonry wall cross sectional area,  $f_y$  is the yield strength of the vertical bars (500 and 450 MPa for *Buildings III* and *IV*, respectively),  $f'_m$  is the masonry compressive strength (19 and 17 MPa for *Buildings III* and *IV*, respectively) and  $P$  is the axial load on the wall.

$$I_e = \alpha I_g \quad \alpha = \left( \frac{100}{f_y} + \frac{P}{f'_m A_g} \right) \quad (2)$$

In Equation (1) a stiffness modifier,  $n$ , of value 10 is used in calculating the rotational stiffness,  $K_\theta$ , because the wall is modeled as a rotational spring connected in series with elastic beam-column element, as shown in Figure 6. Subsequently, the stiffness of these components is modified so that their equivalent stiffness,  $K_w$ , is equal to the stiffness of the actual wall. For this reason, and also to avoid any numerical problems, the rotational spring stiffness,  $K_\theta$ , and the elastic element stiffness,  $K_e$ , are multiplied by modification factors of  $(n+1)$  and  $(n+1/n)$ , respectively, as suggested by Ibarra and Krawinkler [14], and wall equivalent stiffness,  $K_w$ , is then calculated.

$$K_w = \frac{K_\theta K_e}{K_\theta + K_e} \quad (3)$$

The RC floor slabs of *Buildings III* and *IV* were modelled considering the diaphragm possessing no out-of-plane stiffness, while still being stiff in the in-plane direction.

## MODEL VALIDATION

Figure 7 compares the results of the numerical model with the corresponding experimental results for *Building III* tested by Ashour et al. [6]. The figure shows that the model is capable of simulating most relevant characteristics at different drift levels. The drift ranges in Figure 7 cover the entire load-displacement curve up to degradation to 80% of the ultimate strength. The lateral load of the building is predicted closely for most of the lateral drift levels, with a maximum deviation in the lateral load prediction of less than 13%.



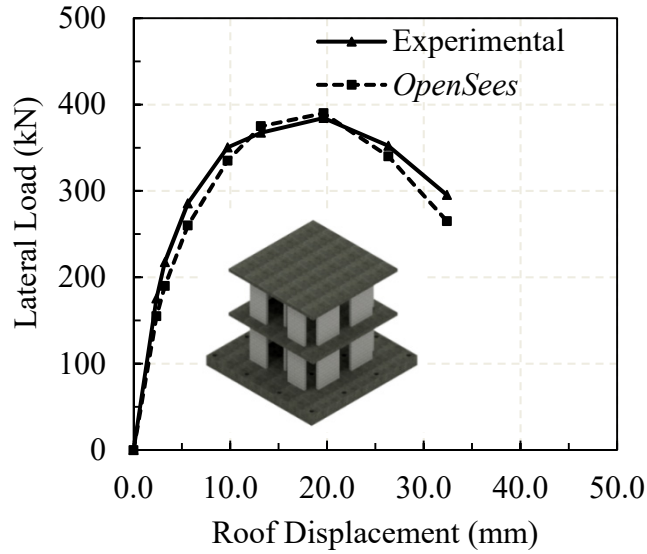


**Figure 7: Experimental and numerical envelopes of *Building III* [6].**

To verify the effectiveness of the developed model for buildings with boundary elements, the model results are compared with the experimental results from *Building IV* [12] in Figure 8. Relative to the experimental results, the maximum error in the lateral load prediction is less than 11%. Overall, the comparison between the experimental and numerical results shows that the proposed model, based on previous results for RC, is capable of capturing the response of RM shear wall buildings both with and without boundary elements.

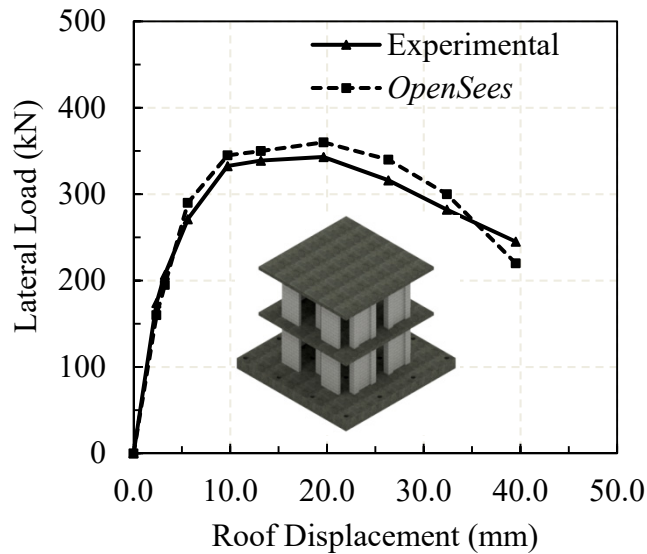


**Figure 8: Experimental and numerical envelopes of *Building IV* [12].**

## CONCLUSIONS

This paper developed a numerical macro model using OpenSees to simulate the behaviour of reinforced masonry shear wall buildings without and with boundary elements. Data from two experimental test programs were used to verify the proposed modelling technique, and it was found that this model is generally able to capture the peak values of cyclic load of the experimental specimens, as well as the strength degradation. This paper demonstrated that reinforced masonry shear walls buildings can be simulated accurately using a simple macro model.

The validations in this paper were limited to two specific configurations of RM shear wall buildings without and with boundary elements. Ongoing research seeks to verify the robustness of the model for different buildings with different aspect ratios. Research is also underway to apply this modelling technique to simulate the hysteretic behaviour of reinforced masonry shear wall buildings under cyclic loading.

## ACKNOWLEDGMENTS

The financial support for this project was provided through the Natural Sciences and Engineering Research Council (NSERC) of Canada and the Canada Masonry Design Centre (CMDC). Support was also provided by the McMaster University Centre for Effective Design of Structures (CEDS), funded through the Ontario Research and Development Challenge Fund (ORDCF) of the Ministry of Research and Innovation (MRI).

## REFERENCES

- [1] Mojsilovic, N., and Marti, P. (1997). "Strength of masonry subjected to combined actions." *ACI structural journal*, 94(6), 633-642.
- [2] Ezzeldin, M., Wiebe, L., and El-Dakhakhni, W. (2016). "Seismic collapse risk assessment of reinforced masonry walls with boundary elements using the FEMA P695 methodology." *J. Struct. Eng.*, 142(11), 04016108.
- [3] Marques, R., and Lourenço, P. B. (2014). "Unreinforced and confined masonry buildings in seismic regions: Validation of macro-element models and cost analysis." *Engineering Structures*, 64, 52-67.
- [4] ATC (Applied Technology Council) (2010). "Modeling and acceptance criteria for seismic design and analysis of tall buildings." *PEER/ATC Report No. 72-1*, Redwood City.
- [5] Priestley, N., Calvi, G., and Kowalsky, M. (2007). *Displacement-Based Seismic Design of Structures*, IUSS Press, Pavia, Italy.
- [6] Ashour, A., El-Dakhakhni, W., and Shedid, M. (2016). "Experimental evaluation of the system-level seismic performance and robustness of an asymmetrical reinforced concrete block building." *J. Struct. Eng.*, 04016072.
- [7] Canadian Standards Association (CSA). (2014). *Design of masonry structures*, CSA S304-14, Mississauga, Canada.
- [8] The Masonry Society (TMS). (2016). *Building code requirements and specifications for masonry structures*, TMS 402/602-16, the Masonry Society, American Society of Civil Engineers, Boulder, New York/American Concrete Institute, and Detroit, USA.

- [9] Shedid, M. T., El-Dakhakhni, W. W. and Drysdale, R. G. (2010). "Alternative strategies to enhance the seismic performance of reinforced concrete-block shear wall systems." *J. Struct. Eng.*, 136(6), 676-689.
- [10] Banting, B. R. and El-Dakhakhni, W. W. (2012). "Force- and displacement-based seismic performance parameters for reinforced masonry structural walls with boundary elements." *J. Struct. Eng.*, 138(12), 1477-1491.
- [11] McKenna, F., Fenves, G. L., and Scott, M. H. (2000). *Open system for earthquake engineering simulation*, Univ. of California, Berkeley, Calif., <http://opensees.berkeley.edu>.
- [12] Ezzeldin, M., El-Dakhakhni, W., and Wiebe, L. (2016c). "System-level seismic performance assessment of an asymmetrical reinforced concrete block building with boundary elements." *16<sup>th</sup> International Brick and Block Masonry conf.*, Padova, Italy.
- [13] ASCE/SEI (Structural Engineering Institute). (2014). "Seismic Evaluation and Retrofit of Existing Buildings." *ASCE/SEI 41-13*, Reston, VA.
- [14] Ibarra, L. F., and Krawinkler, H. (2005). "Global collapse of frame structures under seismic excitations." Berkeley, CA: *Pacific Earthquake Engineering Research Center*.
- [15] Paulay, T., and Priestly, M. (1992). *Seismic design of reinforced concrete and masonry buildings*, Wiley, New York.